

## Pressure tuned ferroelectric reentrance in nano-BaTiO<sub>3</sub> ceramics

J. L. Zhu, S. Lin, S. M. Feng, L. J. Wang, Q. Q. Liu et al.

Citation: *J. Appl. Phys.* **112**, 124107 (2012); doi: 10.1063/1.4770358

View online: <http://dx.doi.org/10.1063/1.4770358>

View Table of Contents: <http://jap.aip.org/resource/1/JAPIAU/v112/i12>

Published by the [American Institute of Physics](#).

---

### Related Articles

Electric field induced polarization and strain of Bi-based ceramic composites

*J. Appl. Phys.* **112**, 124109 (2012)

Nonlinear dielectric response in piezoelectric materials for underwater transducers

*J. Appl. Phys.* **112**, 124108 (2012)

Upconversion luminescence, ferroelectrics and piezoelectrics of Er Doped SrBi<sub>4</sub>Ti<sub>4</sub>O<sub>15</sub>

*AIP Advances* **2**, 042187 (2012)

The dominance of paramagnetic loss in microwave dielectric ceramics at cryogenic temperatures

*Appl. Phys. Lett.* **101**, 252901 (2012)

Phase transitions and electromechanical properties for barium titanate and lead titanate ferroelectric crystals under one-dimensional shock wave compression

*J. Appl. Phys.* **112**, 114118 (2012)

---

### Additional information on *J. Appl. Phys.*

Journal Homepage: <http://jap.aip.org/>

Journal Information: [http://jap.aip.org/about/about\\_the\\_journal](http://jap.aip.org/about/about_the_journal)

Top downloads: [http://jap.aip.org/features/most\\_downloaded](http://jap.aip.org/features/most_downloaded)

Information for Authors: <http://jap.aip.org/authors>

## ADVERTISEMENT



**AIP Advances**

Now Indexed in Thomson Reuters Databases

Explore AIP's open access journal:

- Rapid publication
- Article-level metrics
- Post-publication rating and commenting

## Pressure tuned ferroelectric reentrance in nano-BaTiO<sub>3</sub> ceramics

J. L. Zhu,<sup>1</sup> S. Lin,<sup>1</sup> S. M. Feng,<sup>1</sup> L. J. Wang,<sup>1</sup> Q. Q. Liu,<sup>1</sup> C. Q. Jin,<sup>1,a)</sup> X. H. Wang,<sup>2,a)</sup>  
 C. F. Zhong,<sup>2</sup> L. T. Li,<sup>2</sup> and Wenwu Cao<sup>3</sup>

<sup>1</sup>The Institute of Physics, Chinese Academy of Sciences, P.O. Box 603, Beijing 100190, China

<sup>2</sup>Department of Materials Sciences, Tsinghua University, Beijing 100084, China

<sup>3</sup>Materials Research Institute, The Pennsylvania State University, University Park, Pennsylvania 16802, USA

(Received 6 October 2012; accepted 19 November 2012; published online 20 December 2012)

In nano-grain BaTiO<sub>3</sub> ceramics, internal compressive stresses make the cubic phase more stable, while internal shear stresses stabilize rhombohedral and orthorhombic phases. The competition between internal compressive stresses and internal shear stresses gives a ferroelectric to paraelectric to ferroelectric reentrance phenomenon as a function of grain size. The pressure can be a tuning factor of reentrance behavior by controlling the interactions between external hydrostatic pressure and internal compressive stresses. These experimental phenomena can be well described by a modified Ginzburg-Landau-Devonshire thermodynamic theory. © 2012 American Institute of Physics. [<http://dx.doi.org/10.1063/1.4770358>]

### INTRODUCTION

As a classical ferroelectric material, BaTiO<sub>3</sub> (BTO) has attracted great interests among engineers and scientists because of its applications in multilayer ceramic capacitors and ferroelectric memories, or its unique characteristics for theoretical studies. In the nano-meter scale, BTO ceramic exhibits some distinctive properties, especially the change of dielectric properties and the shift of phase transition temperatures.<sup>1–4</sup> There are also some theoretical investigations on size effects in BTO systems based on different theoretical models.<sup>5–13</sup>

In previous investigations,<sup>14,15</sup> we have systematically studied nano size effect in BTO ceramic systems, which results in the decrease of the Curie temperature  $T_C$  for the cubic to tetragonal phase transition and the increase of rhombohedral to orthorhombic ( $T_2$ ) and orthorhombic to tetragonal ( $T_1$ ) phase transition temperatures. By assuming grains in dense nanoceramics to be in single domain state and using the Core-shell model in Ginzburg-Landau-Devonshire (GLD) thermodynamic theory, Lin *et al.*<sup>14</sup> successfully explained the decrease of  $T_C$  and the increase of  $T_1$  and  $T_2$  based on internal compressive stresses and internal shear stresses, the competition between the two stresses caused the ferroelectric reentrance phase boundary. In this work, the predicted ferroelectric reentrance phenomenon<sup>14</sup> is confirmed by the newly updated experimental data. In addition, we have further modified the phenomenological theory by including the hydrostatic pressure, internal compressive stresses, internal shear stresses, and the interactions of hydrostatic pressure with internal compressive stresses. The internal shear stresses part was also enlarged to better describe the experimental data. The modified model can quantitatively explain the experimentally observed ferroelectric reentrance phenomenon and the shift of  $T_C$  under pressure with grain size down to 15 nm. The ferroelectric reentrance

phenomenon provides a good explanation to why there is still ferroelectricity in nano-BTO ceramics when the grain size is as small as 15 nm, whereas for BTO nano-powders, the ferroelectricity disappeared when the particle size is approaching 30 nm.<sup>7,8</sup> From the improved GLD model, we also predicted the rate of  $T_1$  change caused by external pressure.

Based on previous experimental results on nano-BTO ceramic,<sup>16–20</sup> a grain size dependence of  $T_C$  is plotted in Figure 1. The theoretical prediction<sup>14</sup> is also shown in Figure 1 by the dashed line. One can see that the critical grain size, at which the ferroelectric reentrance phenomenon of nano-BTO happens, is inconsistent between the experimental observation and the GLD theoretical prediction. This might be caused by the lack of reliable experimental data for nano-BTO ceramics with grain size smaller than 20 nm and the less accurate parameters used in that theory model. In order to resolve this issue, smaller size (less than 20 nm) BTO ceramic needs to be fabricated.

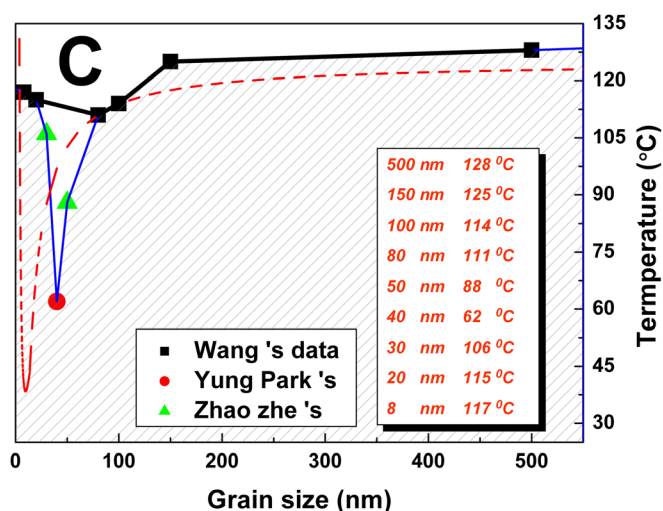


FIG. 1. Dependence of the Curie temperatures  $T_C$  on grain size. The symbol points are experimental data, solid lines are guide for the eyes and the dashed line is the GLD calculation reproduced from Ref. 14.

<sup>a)</sup>Authors to whom correspondence should be addressed. Electronic addresses: JIN@iphy.ac.cn and wxh@tsinghua.edu.cn.

It was found that different synthesis methods and different Ba/Ti ratios can produce different  $T_C$  for the same grain size BTO ceramic samples.<sup>21,22</sup> Therefore, it is not appropriate to analyze the reentrance phenomenon using different author's data. If we only consider the data produced by the same group,<sup>17,19,20</sup> distinct reentrance phenomenon can be seen as shown in Figure 1. In order to minimize the influence of synthesis process and Ba/Ti ratio effect,<sup>18,21</sup> we used the same initial BTO nano powders and synthesize all the samples with grain size of 100 nm, 60 nm, and 15 nm using the exact two stage<sup>23</sup> solid state reaction method under high pressure. In this work, we report the temperature dependence of the dielectric constant and the change of the cubic to tetragonal ( $C$ - $T$ ) phase transition temperature for the 15 nm grain size BTO ceramic under hydrostatic pressure.

## EXPERIMENTAL

The temperature dependence of the dielectric constant of BTO ceramic was measured under a pressure from ambient up to 5 GPa at  $10^5$  Hz using an electrical impedance analyzer (HP 4192A). The temperature and dielectric constant values were recorded by a personal computer in an automated measurement set-up. The electrodes on the samples were prepared by applying a thin coating of Ag paint on the two parallel planes of each sample. During the experiment, the sample was placed in the center of a pyrophyllite cube ( $25 \times 25 \times 25$  mm<sup>3</sup> in size) surrounded by a pressure transmitting medium (boron nitride). To maintain the hydrostatic pressure environment, the sample was shaped into a smaller but more regular geometry with 3 mm in diameter and 1 mm in thickness. A Cu wire of 0.1 mm in diameter encapsulated by a Teflon tube was used to make a flexible contact with the sample at the diagonal corners of the pyrophyllite cube and external leads were screened by copper metal net. The sample was in a graphite tube served as the heater and two metal pellets attached to the top and bottom anvils as the contacts for the electric circuit. Temperature was monitored by a NiCr-NiSi thermocouple mounted very close to the sample. The pyrophyllite cube was placed in the center cavity of the cubic anvil apparatus that can generate pressure up to 6 GPa.

## RESULTS AND DISCUSSIONS

With the updated experimental  $T_C$  data for the 15 nm BTO ceramic under different pressure from ambient up to 2 GPa, we were able to modified the theoretical model by increasing the internal shear stresses effect in the parameter  $\alpha_{12}^*(d)$  and also considered the interaction between hydrostatic pressure and internal compressive stresses in the parameter  $\alpha_1^*(T, d)$ .<sup>14</sup> It is the first time that the hydrostatic pressure, internal compressive stresses as well as internal shear stresses were all included in the GLD model. With such modification, the nano size effect as well as the applied pressure effect of BTO ceramics with grain size down to 15 nm could be quantitatively described by the improved GLD phenomenological theory.

The relative dielectric constant as a function of temperature under different pressure for the 15 nm BTO ceramic in the temperature region of paraelectric-ferroelectric phase

transition is shown in Figure 2. With increasing pressure, the dielectric constant is strongly suppressed and the peak becomes more diffusive. In the pressure range from 0 to 2 GPa,  $T_C$  decreases linearly with pressure, which is an extension to the results of Refs. 24 and 25. The rates of change are  $dT_C/dP = -37.1 (\pm 1.3)$  K/GPa,  $-34.3 (\pm 1.4)$  K/GPa, and  $-23.5 (\pm 1.7)$ , respectively, for 100 nm, 60 nm, and 15 nm grain size BTO ceramic samples.<sup>15</sup>

In the improved GLD model, we have enlarged internal shear stresses part by a factor of 7/6 compared to the original  $\alpha_{12}^*(d)$  used in Ref. 14 (see Eq. (1)), which stabilized the rhombohedral phase. With such a treatment, in the reentrance region, the rhombohedral-cubic phase boundary is shifted to higher temperature. Second, we have considered the interaction between hydrostatic pressure and internal compressive stresses in the parameter  $\alpha_1^*(T, d)$ . This is reflected in Eq. (2), and the variation of  $dT_C/dP$  can now be well described by this improved model.

$$\alpha_{12}^*(d) = \alpha_{12}(T) + \frac{7K_2}{6d}, \quad (1)$$

$$\alpha_1^*(T, \sigma, d) = \alpha_1(T) + \frac{K_1 + SP}{19d}. \quad (2)$$

Figure 3 gives the phase diagram of the transition temperature  $T_C$  versus grain size under different pressure up to 2 GPa. The circles are experimental data for 100 nm, 60 nm, and 15 nm BTO ceramic samples, and the lines are theoretical calculated results. The ferroelectric reentrance phenomenon from ferroelectric phase ( $T$ ) to paraelectric phase ( $C$ ) and then to another ferroelectric phase ( $R$ ) is observed as a function of grain size at a fixed temperature, as indicated by the horizontal arrow in Figure 3. The rhombohedral to orthorhombic and orthorhombic and tetragonal phase boundaries predicted by the theory were only shown for ambient pressure in dash lines.

In this improved GLD model, there are three stresses: internal compressive stresses, internal shear stresses, and hydrostatic pressure. On one hand, the internal compressive

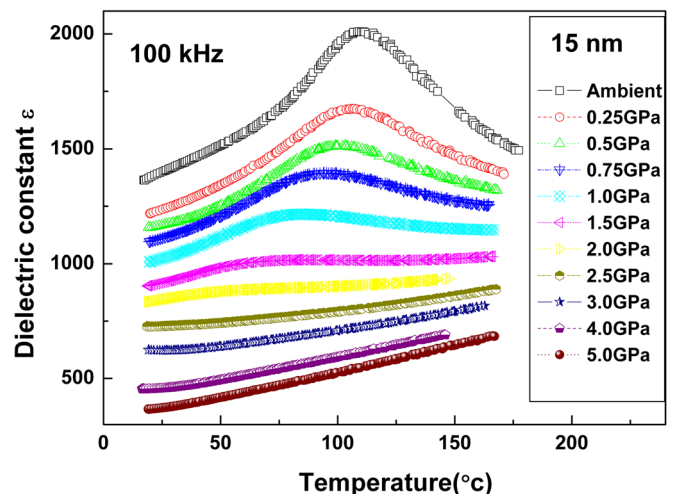


FIG. 2. The relative dielectric constant for the 15 nm BTO ceramic sample as a function of temperature under different pressures in the region of paraelectric to ferroelectric phase transition.

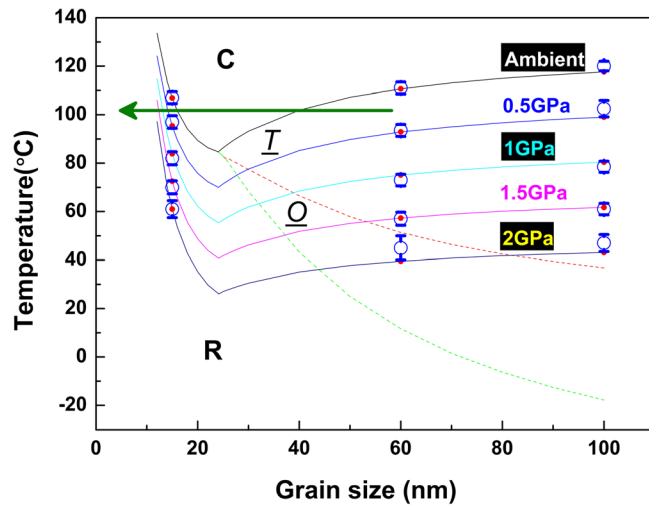


FIG. 3. Phase diagram of the transition temperature versus grain size under pressure from ambient up to 2 GPa. The circles are experimental data for 100 nm, 60 nm, and 15 nm BTO ceramic samples, and the lines are theoretical calculated results. The ferroelectric reentrance phenomenon from ferroelectric tetragonal phase (*T*) to paraelectric cubic phase (*C*) and then to ferroelectric rhombohedral phase (*R*) is observed as a function of grain size at a fixed temperature, as indicated by the horizontal arrow. The rhombohedral to orthorhombic and orthorhombic to tetragonal phase boundaries are only shown for ambient pressure in dashed lines.

stresses favor the cubic phase, so that  $T_C$  shifts to lower temperature with decreasing grain size. On the other hand, the internal shear stresses stabilize the rhombohedral phase, so that  $T_2$  shifts to higher temperature with decreasing grain size. When these two stresses are strong enough, both tetragonal and orthorhombic phases will vanish, hence, the balance between internal compressive stresses and internal shear stresses produces an interesting phase diagram. The ferroelectric to paraelectric to ferroelectric reentrance phenomenon indicates that the dominant one is the internal shear stresses in smaller nano-grain size BTO ceramic samples. If removing the internal shear stresses, the calculated  $T_C$  for the 15 nm BTO ceramic sample will be 61.8 °C, which is significantly lower than the experimentally observed 107 °C.

The  $dT_C/dP$  is controlled by the interactions between internal compressive stresses and hydrostatic pressure. Hydrostatic pressure has influence on internal compressive stresses but not on internal shear stresses. Based on some published works about the influence of stresses on nano-powder and nano-ceramic BTO<sup>5,26</sup> the smaller is the grain size, the stronger is the modification of hydrostatic pressure on internal compressive stresses. The slope amplitude  $|dT_C/dP|$  is smaller for smaller nano-grain size ceramic. If there is no interaction between hydrostatic pressure and internal compressive stresses, the calculated slope  $dT_C/dP$  will be the same for all grain size samples. Figure 4 is the theoretically calculated orthorhombic to tetragonal phase transition temperature  $T_1$  for different grain size BTO ceramic samples under pressure from ambient up to 2 GPa. There is no interaction between hydrostatic pressure and internal shear stresses, so the pressure derivatives of the transition temperature ( $dT_1/dP$ ) are almost the same for all calculated data. This theoretical prediction, of course, awaits for further experimental verification in the future.

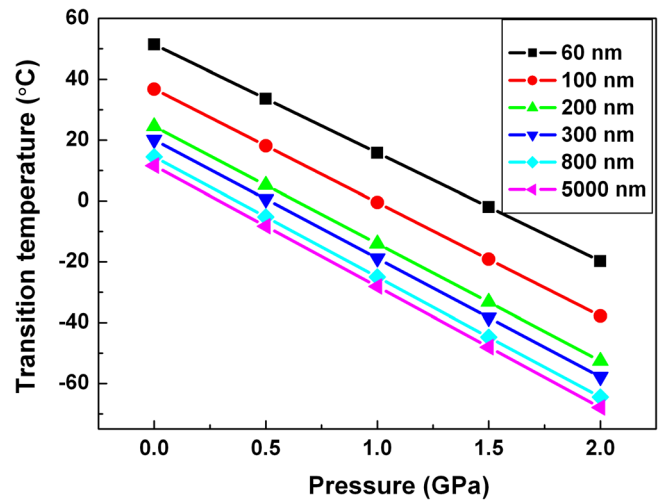


FIG. 4. Theoretically calculated orthorhombic to tetragonal phase transition temperature  $T_1$  for different grain size BTO ceramic samples under pressures from ambient up to 2 GPa. The slopes ( $dT_1/dP$ ) are parallel for different grain size ceramic samples.

In conclusion, in nano BTO ceramic, the internal compressive stresses forces the cubic-tetragonal transition temperature to decrease and the internal shear stresses stabilizes the rhombohedral phase. When the internal compressive stresses and internal shear stresses grow stronger in smaller nano-grain size BTO samples, their combined effect will eliminate the orthorhombic and tetragonal ferroelectric phases, leading to the ferroelectric reentrance phenomenon with rhombohedral phase in nano BTO ceramics. The pressure tuning of the Curie temperature  $T_C$  is controlled by the interaction between hydrostatic pressure and internal compressive stresses.

## ACKNOWLEDGMENTS

This work is supported by NSF & MOST of China through research projects and by the Ministry of Sciences and Technology of China through the 973-Project under Grant No. 2009CB623301 and National Science fund for Creative Research Groups (Grant No. 50921061).

- <sup>1</sup>G. H. Haertling, *J. Am. Ceram. Soc.* **82**, 797 (1999).
- <sup>2</sup>U. D. Venkateswaran, V. M. Naik, and R. Naik, *Phys. Rev. B* **58**, 14256 (1998).
- <sup>3</sup>M. Boulos, S. G. Fritsch, F. Mathieu, B. Durand, T. Lebey, and V. Bley, *Solid State Ionics* **176**, 1301 (2005).
- <sup>4</sup>Y. C. Wu, J. S. Lee, H. Y. Lu, and C. L. Hu, *J. Electroceram.* **18**, 13 (2007).
- <sup>5</sup>K. Uchino, E. Sadanaga, and T. Hirose, *J. Am. Ceram. Soc.* **72**, 1555 (1989).
- <sup>6</sup>W. L. Zhong, Y. G. Wang, and P. L. Zhang, *Phys. Lett. A* **189**, 121 (1994).
- <sup>7</sup>S. Aoyagi, Y. Kuroiwa, A. Sawada, H. Kawaji, and T. Atake, *J. Therm. Anal. Calorim.* **81**, 627 (2005).
- <sup>8</sup>F. S. Yen, H. I. Hsing, and Y. H. Chang, *Jpn. J. Appl. Phys., Part 1* **34**, 6149 (1995).
- <sup>9</sup>J. Junquera and P. Ghosez, *Nature (London)* **422**, 506 (2003).
- <sup>10</sup>Y. S. Kim, D. H. Kim, J. D. Kim, Y. J. Chang, T. W. Noh, J. H. Kong, K. Char, Y. D. Park, S. D. Bu, J.-G. Yoon, and J.-S. Chung, *Appl. Phys. Lett.* **86**, 102907 (2005).
- <sup>11</sup>M. Anliker, H. R. Brugger, and W. Kanzig, *Helv. Phys. Acta* **27**, 99 (1954).

- <sup>12</sup>R. Böttcher, C. Klimm, D. Michel, H.-C. Semmelhack, G. Völkel, H.-J. Cläsel, and E. Hartmann, *Phys. Rev. B* **62**, 2085 (2000); E. Erdem, R. Boettcher, H.-J. Glaesel, E. Hartmann, G. Klotzsche, and D. Michel, *Ferroelectrics* **316**, 43 (2005).
- <sup>13</sup>M. D. Glinchuk, and A. N. Morozovskaya, *Phys. Status Solidi B* **238**, 81 (2003); M. D. Glinchuk and P. I. Bykov, *J. Phys: Condens. Matter* **16**, 6779 (2004).
- <sup>14</sup>S. Lin, T. Q. Lü, C. Q. Jin, and X. H. Wang, *Phys. Rev. B* **74**, 134115 (2006).
- <sup>15</sup>J. L. Zhu, C. Q. Jin, W. W. Cao, and X. H. Wang, *Appl. Phys. Lett.* **92**, 242901 (2008).
- <sup>16</sup>Y. Parky, W. Lee and H. G. Kim, *J. Phys: Condens. Matter* **9**, 9445 (1997).
- <sup>17</sup>B. R. Li, X. H. Wang, L. T. Li, H. Zhou, X. T. Liu, X. Q. Han, Y. C. Zhang, X. W. Qi, and X. Y. Deng, *Mater. Chem. Phys.* **83**, 23 (2004).
- <sup>18</sup>V. Buscaglia, M. Viviani, M.T. Buscaglia, P. Nanni, L. Mitoseriu, A. Testino, E. Stytsenko, M. Daghli, Z. Zhao, and M. Nygren, *Powder Technol.* **148**, 24 (2004).
- <sup>19</sup>X. Y. Deng, X. H. Wang, H. Wen, L. L. Chen, L. Chen, and L. T. Li, *Appl. Phys. Lett.* **88**, 252905 (2006).
- <sup>20</sup>X. H. Wang, X. Y. Deng, H. Wen, and L. T. Li, *Appl. Phys. Lett.* **89**, 162902 (2006).
- <sup>21</sup>Z. Zhao, V. Buscaglia, M. Viviani, M. T. Buscaglia, L. Mitoseriu, A. Testino, M. Nygren, M. Johnsson, and P. Nanni, *Phys. Rev. B* **70**, 024107 (2004).
- <sup>22</sup>S. Lee, Z. K. Liu, and M. H. Kim, *J. Appl. Phys.* **101**, 054119 (2007).
- <sup>23</sup>I. W. Chen and X. H. Wang, *Nature* **404**, 168 (2000).
- <sup>24</sup>W. J. Merz, *Phys. Rev.* **78**, 52 (1950).
- <sup>25</sup>T. Ishidate, S. H. Takahashi, and N. Môri, *Phys. Rev. Lett.* **78**, 2397 (1997).
- <sup>26</sup>G. Arlt, D. Henning, and G. de With, *J. Appl. Phys.* **58**, 1619 (1985).